JOURNAL OF SOLID STATE CHEMISTRY 49, 134–149 (1983)

Vibrational Study of the $[P_2S_6^{4-}]$ Anion, of Some MPS_3 Layered Compounds (M = Fe, Co, Ni, $In_{2/3}$), and of Their Intercalates with $[Co(\eta^5\text{-}C_5H_5)_2^+]$ Cations

C. SOURISSEAU AND J. P. FORGERIT

Laboratoire de Spectrochimie Infrarouge et Raman, CNRS, 94320 Thiais, France

AND Y. MATHEY

Laboratoire de Physicochimie Minérale et ERA 672, Université de Paris Sud, 91405 Orsay, France

Received November 30, 1982, and in revised form March 28, 1983

The infrared and Raman spectra [10–3100 cm^{-1}] have been recorded for aqueous solutions and polycrystalline samples of $Na_4P_2S_6 \cdot 6H_2O$ as well as for several lamellar MPS_3 (or $M_2P_2S_6$) compounds with M = Fe, Co, Ni, $In_{2/3}$ and their intercalates with cobalticenium cations. A complete assignment of the observed spectra is proposed and a normal coordinate analysis of the $[P_2S_6^{4-}]$ anion is carried out; this allows proposal of a new assignment, for the spectra of the layered MPS_3 host systems which is slightly modified with respect to prior work. A detailed analysis of the infrared and far-infrared spectra is also reported for the intercalates with $[Co(\eta^5\text{-}C_5H_5)_2^+]$ cations. From these results, it is concluded that the mechanism of the electronic transfer during the intercalation process depends on the nature of the metal: when M = Co or Ni the main reduction site is the P–P bond, while when M = Fe (and perhaps also Mn) the reduction involves mainly the metal ion itself.

Introduction

The broadband semiconductors metal hexathiohypodiphosphates of general formula MPS_3 (M = first row transition metal) are structured on the same general pattern as the two-dimensional MS_2 systems; the stacking of the $SM_{2/3}(P_2)_{1/3}S$ slabs gives rise to Van der Waals' gaps in which cations can be intercalated (*1, 2*). These intercalation compounds are of interest because of their quasi-two-dimensional properties and of their applications as electrodes in high energy density batteries (*3*).

As a part of a general vibrational study of these lamellar materials intercalated with organometallic cations, we have recently shown for $MnPS_3$, $ZnPS_3$, and $CdPS_3$ systems that structural and dynamic information can be obtained by infrared, Raman, and inelastic neutron scattering spectroscopy (*4–8*). The present study is more precisely concerned with the vibrational spectra of $FePS_3$, $CoPS_3$, and $NiPS_3$ compounds which are strongly colored semiconductors with gaps of about 1.5 eV. Among these chalcogenophosphates, $NiPS_3$ and, to a lesser degree, $FePS_3$ behave as good cathode materials in lithium batteries (*3, 9, 10*). In addition the spectra of the corresponding

[1] To whom all correspondence should be addressed.

0022-4596/83 $3.00

intercalates with $Co(\eta^5\text{-}C_5H_5)_2$ (denoted hereafter $CoCp_2$) are investigated. In order to confirm some vibrational assignments, a complete infrared and Raman study and a normal coordinate analysis of the [$P_2S_6^{4-}$] anion existing in $Na_4P_2S_6 \cdot 6H_2O$ are also carried out. Furthermore, the spectra of the metal-deficient layered compound $In_{2/3}\square_{1/3}PS_3$ (where $\square$ stands for metal vacancies) are presented in order to understand the effects of a multiplicity increase ($Z \times 3$) in the layer planes (*11, 12*). Finally, an important goal of this optical study of the cobalticenium intercalates is to examine the electronic perturbations induced by the electron transfer which has occurred from the organometallic species to the inorganic host lattice during the intercalation process.

Experimental

I. Experimental Procedure

$Na_4P_2S_6 \cdot 6H_2O$ was synthesized by slow addition of PCl_3 to an aqueous solution of Na_2S, following the procedure described by H. Falius (*13*). Well-shaped, colorless crystals were obtained by recrystallization of the initial polycrystalline precipitate from a water–ethanol mixture.

Analyses. $Na_4P_2S_6 \cdot 6H_2O$. Calcd: Na, 20.2; P, 13.6; S, 42.3; H, 2.7. Found: Na, 19.7; P, 13.6; S, 40.3; H, 3.1.

The layered systems MPS_3 with M = Fe, Co, Ni, and $In_{2/3}$ were synthesized according to existing procedures (*11, 14, 15*) and were characterized by means of X-ray powder diffraction and chemical analysis. Intercalation in M = Fe, Co, Ni host systems was performed via the classical or "direct" route, i.e., by treating the pure materials with a toluene solution of cobaltocene for ~3 days at about 120°C in Pyrex ampoules sealed under vacuum (*16*). It should be mentioned here that no intercalation was observed after several weeks of treating the same starting materials with aqueous or alcoholic solutions of cobalticenium iodide, a route of intercalation which has been proved to be successful with M = Mn, Zn, or Cd materials (*17*).

For the $In_{2/3}\square_{1/3}PS_3$ system, it is noted that a complete, well-characterized, intercalation could not be achieved, whatever route, solvent, and temperature conditions that were adopted. Therefore, no special study will be reported here.

The sets of (00*l*) lines observed in the X-ray powder diffraction patterns demonstrate that the interlayer distance increases by 5.32, 5.40, and 5.33 Å upon intercalation of cobalticenium in $FePS_3$, $CoPS_3$, and $NiPS_3$, respectively, an increment which satisfactorily compares with the Van der Waals bulk of the cobalticenium cation.

Analyses. $FePS_3(CoCp_2)_{0.37}$. Calcd: Fe, 22.1; P, 12.2; S, 38.0; Co, 8.6; C, 17.5; H, 1.5. Found: Fe, 21.4; P, 12.0; S, 37.4; Co, 8.3; C, 17.2; H, 1.7.

$CoPS_3(CoCp_2)_{0.39}$. Calcd: Co, 31.5; P, 11.9; S, 37.0; C, 18.0; H, 1.5. Found: Co, 31.0; P, 11.0; S, 31.1; C, 14.7; H, 1.7.

$NiPS_3(CoCp_2)_{0.37}$. Calcd: Ni, 23.0; P, 12.1; S, 37.5; Co, 8.5; C, 17.3; H, 1.5. Found: Ni, 23.0; P, 12.1; S, 36.3; Co, 8.1; C, 17.6; H, 1.6.

$In_{2/3}\square_{1/3}PS_3$. Calcd: In, 37.6; P, 15.2; S, 47.2. Found: In, 39.7; P, 14.4; S, 46.6.

Almost all the compounds under study seem to be stable in air; their spectra have been recorded without protecting the samples from the atmosphere. In the particular case of the $CoPS_3$ intercalate, chemical analyses performed on the powder samples show discrepancies with respect to the calculated formula. This feature may be attributed in part to small amounts of CoS_2 and/or $Co_3(PS_4)_2$ phases present as impurities, as mentioned in (*15*) but an extensive oxidation of the host system cannot be ruled out. Therefore infrared spectra were recorded using freshly prepared samples.

II. Spectra

In sharp contrast with the optical characteristics encountered with the MPS_3 compounds of Mn, Zn, Cd, the reflectivity and opacity of the dark systems under study, excepting $Na_4P_2S_6 \cdot 6H_2O$ and $In_{2/3}\square_{1/3}PS_3$, render the Raman scattering experiments and the infrared absorption recordings rather difficult. Part of the experimental difficulties inherent in dealing with these optically poor samples have been overcome in the following manner.

—Raman spectra were obtained by accumulation with a computerized triple monochromator CODERG T800 instrument using a krypton (647.1 nm) and an argon (514.5–488.0 nm) laser in conjunction with a glass block rotating at 1500 rpm in order to avoid any decomposition. Furthermore, some spectra were also recorded with a Raman microprobe double monochromator Jobin Yvon Mole instrument using an argon laser.

—Infrared spectra were recorded on Perkin–Elmer 225 and 180 spectrometers and on a Polytec Fir 30 interferometer. Monocrystalline platelets were examined using a beam condenser; the polycrystalline samples were dispersed in Nujol.

—Low temperature measurements were obtained using conventional cryostats working with either liquid nitrogen or liquid helium.

Results and Discussion

I. Vibrational Spectra and Normal Coordinate Analysis of the $[P_2S_6^{4-}]$ Anion

In the sodium salt $Na_4P_2S_6$, prepared as an hexahydate, the existence of a $[P_2S_6^{4-}]$ anion of D_{3d} symmetry has been established through ^{31}P-NMR and preliminary X-ray results (*13*). For such ethane-type anions a particularly simple vibrational spectrum is to be expected:

$$\Gamma_{vib}^{D_{3d}} = (3A_{1g} + 3E_g) + 1A_{1u} + (2A_{2u} + 3E_u);$$

six modes are Raman active (the gerade ones) and only five modes are infrared ac-

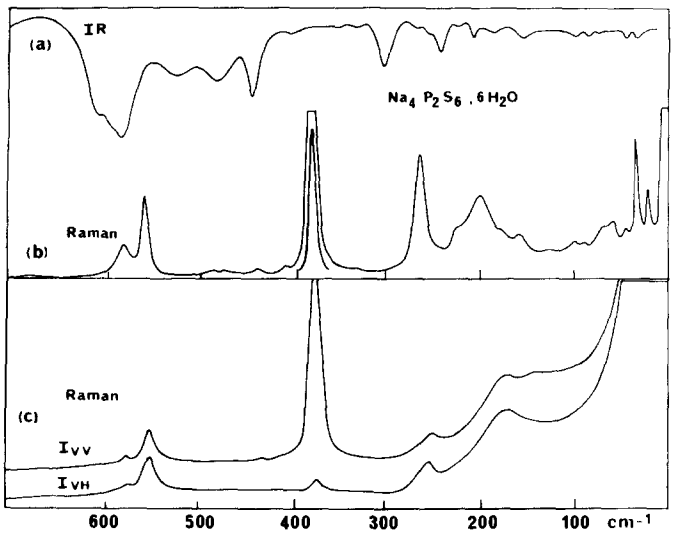

FIG. 1. Room temperature vibrational spectra of the $[P_2S_6^{4-}]$ anion: Infrared (trace a) and Raman (trace b) spectra [700–10 cm^{-1}] for polycrystalline $Na_4P_2S_6$, $6H_2O$ compound. Polarized Raman spectra for aqueous solutions of the sodium salt (curves c).

TABLE I

INFRARED AND RAMAN BAND WAVENUMBERS OF $Na_4P_2S_6 \cdot 6H_2O$: CALCULATED FREQUENCIES OF THE $P_2S_6^{4-}$ ION AND POTENTIAL ENERGY DISTRIBUTIONS (PED)[a]

Bürger and Falius (*18*) Solid, 300 K		This work							
		Solid, 300 K			Calcd.				Number and sym. (D_{3d})
ir	R	ir	R	Soln H_2O	ir	R	PED (%)	Assignment	
606 sh		606 s					Comb. 300 × 2 = 600		
		592 sh					Comb. 443 + 154 = 597		
585 vs	578 m	582 vs	580 m	578 m	587.2		88 ($\nu_d^0PS_3$)		ν_7 (E_u)
	557 s		557 s	553 s		564.5	94 ($\nu_d^pPS_3$) +	Fermi reson. with 376 + 175 = 551	ν_{10} (E_g)
528 vw		525 w							
489 vw		479 w	482 vw	—				Libration (H_2O)	
			475 vw						
444 s		443 m	439 vw	435 w (P)		434.6	100 (νP–P)		ν_3 (A_{1g})
380 vw		399 w	408 vw		393.7		100 ($\nu_s^0PS_3$)		ν_5 (A_{2u})
	374 vs	—	378 vs	376 vs (P)		376.9	100 ($\nu_s^pPS_3$)		ν_1 (A_{1g})
302 s		300 m	—		304.5		100 ($\delta_s^0PS_3$)		ν_6 (A_{2u})
	259 s	265 vw	264 s	257 m		261.9	53 ($\delta_d^pPS_3$) + 30ρ_r^p(PS_3)		ν_{11} (E_g)
243 m		240 m	—		236.8		86 ($\delta_d^0PS_3$)		ν_8 (E_u)
		220 vw	222 m						
	197 m	205 w	200 s						
	169 w	182 vw	178 m	175 s		171.2	76 ($\rho_r^pPS_3$) + 20 ($\delta_d^pPS_3$)		ν_{12} (E_g)
		154 w	158 m	150 s (P)		149.1	70 ($\delta_s^pPS_3$) + 40 (νP–P)		ν_2 (A_{1g})
87 w		96 vw	100 vw		104.2		100 ($\rho_r^0PS_3$)		ν_9 (E_u)
		83 w	90 vw						
			67 w					T' (H_2O)	
			59 w						
		40 vw	44 vw						
		29 vw	33 vs					T' (Na^+)	
			21 s						

[a] Abbreviations used for intensities: vs = very strong; s = strong; m = medium; w = weak; vw = weak; sh = shoulder.

tive ($2A_{2u} + 3E_u$). Nevertheless, due to the lack of polarization measurements, the previously published vibrational assignments are in error (*18, 19*).

The infrared and Raman spectra of this compound in the solid state and the polarized Raman spectra for aqueous solutions are shown on Fig. 1. The corresponding band wavenumbers and assignments are given in Table I; they can be compared both with those previously published for the same Na salt (*18*) and with the results of our normal coordinate calculation. In agreement with the selection rule predictions, the Raman spectra of solutions exhibit only three polarized bands at 435 cm^{-1} (very weak), 376 cm^{-1} (very strong), and 150 cm^{-1} (strong). These bands can be confidently assigned, by comparison with the isoelectronic Si_2Cl_6 molecule (*20*), to the symmetric ν(P–P), $\nu_s(PS_3)$, and $\delta_s(PS_3)$ A_{1g} modes, respectively. The three remaining intense bands at 553, 257, and 175 cm^{-1} must therefore correspond to the stretching, deformation, and rocking E_g modes, respectively. It is noteworthy that the former band is split into two components at 578 and 553 cm^{-1}; this can be explained by the existence of a Fermi resonance with the combination 376 + 175 = 551 cm^{-1}; as both components are depolarized, the previously reported assignments of one of these bands to a symmetric stretching mode are wrong (*18, 19*).

In the Raman spectrum of the solid compound, the same features are observed, with additional weak bands arising from librational motions of H_2O molecules, and also with many new low frequency bands which are assigned to translations of H_2O and Na^+ species (Table I). Similarly, the infrared spectrum can be readily understood: the A_{2u} modes are localized at about 400 and 300 cm^{-1} and the bands at about 582, 240, and 100 cm^{-1} are assigned to the E_u vibrations. In this spectrum, the degenerate stretching PS_3 mode gives rise to a strong and broad absorption band with maxima at 606, 592, and 582 cm^{-1} due to the possible occurrence of many combination bands in this range; moreover, one notes that some vibrations, such as the ν(P–P) mode, become infrared active due to crystal effects.

TABLE II

NON-ZERO SYMMETRY FORCE CONSTANTS (10^2 Nm^{-1} and 10^2 N m/rad) OF THE $P_2S_6^{4-}$ ION

$F_{i,j}$[a]	Value	$F_{i,j}$[a]	Value
1,1 = 5,5	2.67	2,3	−0.40
2,2 = 6,6	1.30	7,7 = 10,10	2.40
3,3	1.85	8,8 = 11,11	1.20
1,2 = 5,6	0.50	9,9 = 12,12	0.90
1,3	0.50	7,9 = 10,12	0.50

[a] Labeling of force constants according to the last column of Table I.

Using the above results, a complete normal coordinate analysis has been performed for the four A_{1g}, A_{2u}, E_u, and E_g blocks with a set of 10 non-zero symmetry force constants (Table II). All the calculated frequencies compare nicely with the observed values, and the potential energy distributions are in satisfactory agreement with our predictions. One notes, however, some vibrational coupling between the $\delta_s(PS_3)$ and ν(P–P) modes in the A_{1g} block and between the $\delta_d(PS_3)$ and $\rho(PS_3)$ vibrations in the E_g blocks (Table I).

Finally, the values of some internal force constants are compared in Table III with those in selected molecules such as $[PS_4^{3-}]$ (*18, 21*), $[P_4S_8]^{4-}$ (*21*), P_4 (*22*) and P_2 (*23*). The P–S stretching force constant, 2.5 × 10^{-2} N m^{-1}, appears to be "normal," as compared with the values known for the $[PS_4^{3-}]$ anion, the upper limit, 2.8 × 10^{-2} N m^{-1}, being observed for $[P_4S_8^{4-}]$ entities; our value for the P–P force constant, 1.85 × 10^{-2} N m^{-1}, marks the lower limit for known P–P bonds and corresponds exactly with that proposed by Somayajulu (*23*) for a

TABLE III

COMPARISON OF SOME INTERNAL FORCE CONSTANTS (10^2 N m^{-1} and 10^2 N m/rad) OF SELECTED MOLECULES

	Ref.	f(PS)	f(PS/PS')	f(PP)	f(SPS')	$f\left(\frac{SPS'}{SPS''}\right)$	f(SPP)
$P_2S_6^{4-}$	This work	2.49	0.09	1.85	1.23	0.03	~0.90
	(*19*)	2.60	0.23	1.60	1.75	—	1.10
	(*18*)	2.70	0.10	2.15	—	—	—
PS_4^{3-}	(*18, 19, 21*)	2.50–2.70	0.27–0.19	—	0.88	0.09	
$P_4S_8^{4-}$	(*21*)	2.80	0.30	2.05			
P_4	(*22*)	—	—	2.065	—	—	
P_2	(*23*)	—	—	1.85	—	—	

single bond. These results show the predominance of P–S bond strengths over P–P interactions in the isolated [$P_2S_6^{4-}$] anions; such a conclusion could not have been reached from a simple comparison of internuclear distances.

II. Vibrational Spectra of the $FePS_3$, $CoPS_3$, and $NiPS_3$ Host Lattices

The crystal structure of these layer-type compounds is known only for $FePS_3$ (*24*). It consists of two layers of sulfur atoms which are in cubic close-packed arrangements with P_2 groups and of metal ions in octahedral sites (Fig. 2). These sandwiches are weakly bonded together, giving rise to Van der Waals' gaps (~3.4 Å), with each layer parallel to the (x, y) planes of the monoclinic structure. The structure belongs to the $C2/m$ (C_{2h}^3) space group with two $FePS_3$ entities per primitive cell. Cobalt and nickel derivatives have nearly the same lattice parameters as $FePS_3$; one may therefore assume isomorphous structures. All the normal modes can be classified according to the representation for $\mathbf{k} = 0$, $\Gamma_{vib}^{C_{2h}} = 8A_g + 7B_g + 6A_u + 9A_u$; one expects 15 Raman and 12 infrared active modes after subtraction of the acoustic modes ($A_u + 2B_u$). However, few intense ir and Raman bands are observed on the recorded vibrational spectra of these compounds (Fig. 3). Also a great similarity with the spectra of the sodium compound $Na_4P_2S_6 \cdot 6H_2O$ is observed: this arises from the existence of [$P_2S_6^{4-}$] entities within the layers; nevertheless, these anions are no longer isolated and, as we have already shown (*4*), it is more appropriate to describe these layered structures as composed of PS_3 groups (d(P–S) ~ 2.0 Å) defining flat pyramids of nearly D_{3h} symmetry, weakly interacting through P–P bonds of length of 2.2 Å. Using the oriented gas model approximation

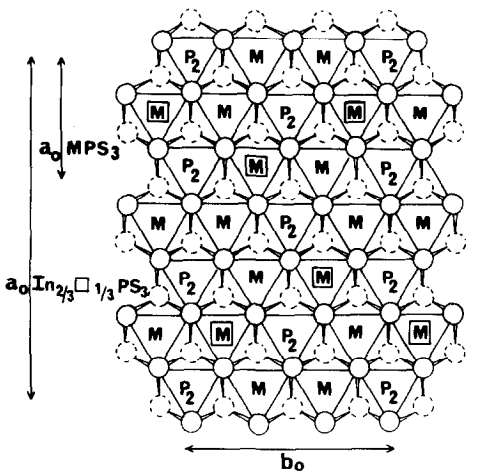

FIG. 2. Schematic representation of the regular (or $FePS_3$-type) and metal-deficient (or $In_{2/3}\square_{1/3}PS_3$-type) structures viewed perpendicular to the layers. In the former case M represents a metal in the formal oxidation state (2+); in the latter, M represents an In^{3+} ion and $\boxed{M}$ designates a vacancy; P_2 denotes P–P pairs.

and the assumption of weak site effects, only eight strong Raman bands and roughly four strong infrared bands are thus expected (*4, 5*).

The infrared and Raman spectra of these compounds are shown on Fig. 3 and the corresponding band wavenumbers are given in Table IV. In the high frequency range (600–150 cm^{-1}) all the bands are assigned in terms of motions of PS_3 groups; one notes that the ν(P–P) mode or the out-of-phase $T'_z(PS_3)$ motion gives rise only to an infrared band at about 440 cm^{-1}, which is in agreement with predictions based on the above selection rules. Similar results have already been obtained for $MnPS_3$, $ZnPS_3$, $CdPS_3$ (*4, 5*), and $Sn_2P_2S_6$ (*25, 26*). According to the above results for $Na_4P_2S_6$, some other band assignments are modified; in particular, we now assign the bands at about 154 cm^{-1} to a symmetric deformation of the PS_3 groups. The important difference between the cation and the PS_3 group masses and the weak interaction between the six sulfur atoms surrounding each metal ion result in a very large separation of the bands responsible for the metal–S and P–S valence vibrations. The few low frequency bands observed at $\nu \leq 140$ cm^{-1} are thus assigned to translational motions of metal ions (Table IV). When we note small frequency variations of these modes within the triad Fe–Co–Ni; for $NiPS_3$, we clearly observe, for the first time, the three expected bands with appreciable Raman intensities. This result indicates the rather covalent character of the Ni–S bonds; this may be linked to recent work where it is stated that the best energy yields in lithium batteries are obtained with low ionicity materials (*10*).

Finally, the large separation (~50–60 cm^{-1}) of these T' modes shows that the metal ions are in anisotropic environments and that the six sulfur atoms surrounding them define strongly distorted octahedra. In fact, the existence of different P–S bonds in these layered structures is also illustrated by a comparison of the infrared spectra for a powder sample and for a monocrystalline platelet (**E**//*ab*) of $CoPS_3$ (Fig. 4): the polarized spectrum shows many absorption maxima on the asymmetric profile of the broad band at about 550–600 cm^{-1} assigned to the $\nu_d(PS_3)$ vibrations. In agreement with structural consider-

TABLE IV

INFRARED AND RAMAN BAND WAVENUMBERS (cm^{-1}) OF SOME MPS_3 COMPOUNDS AT 300 K

$MnPS_3$(4)		$FePS_3$		$CoPS_3$		$NiPS_3$		Approximate type of motions
ir	R	ir	R	ir	R	ir	R	
	579 m	580 sh			605 vw	589 sh		
572 vw	566 w	571 vw	573 w	569 vw	583 w	575 vw	562 s	$\nu_d(PS_3)$
		560 sh	560 vw		556 w	571 sh		
530 w	539 vw	—	544 vw	—	—	—	542 w	Combination
							530 w	
450 m	—	445 w	—	443 w	—	440 w	—	$T'_z(PS_3)$ or ν(P–P)
—	378 vw	—	383 vw	—	378 vw	—	377 vw	$\nu_s(PS_3)$
316 m		295 w		297 w	315 w	289 w	298 w	$\delta_s(PS_3)$
	273 vw		275 s		277 w		271 m	
255 s	244 vw	257 s	255 s	256 vw	245 s	265 s	247 vw	$\delta_d(PS_3)$
	225 m	230 w	221 m	—	221 m	214 vw	222 m	
194 s	185 vw	183 s	—	190 vw	—	187 s		ρr or $R'_{xy}(PS_3)$
152 s	154 m	153 s	152 w	156 s		156 sh	153 w	$\delta_s(PS_3)$
138 s		131 sh	122 m	130 w		139 w	126 w	
115 vw	115 w		95 w	109 w		109 w	95 w	$T'M^{2+}$
	110 w							
		76 vw		74 vw		72 w	76 m	

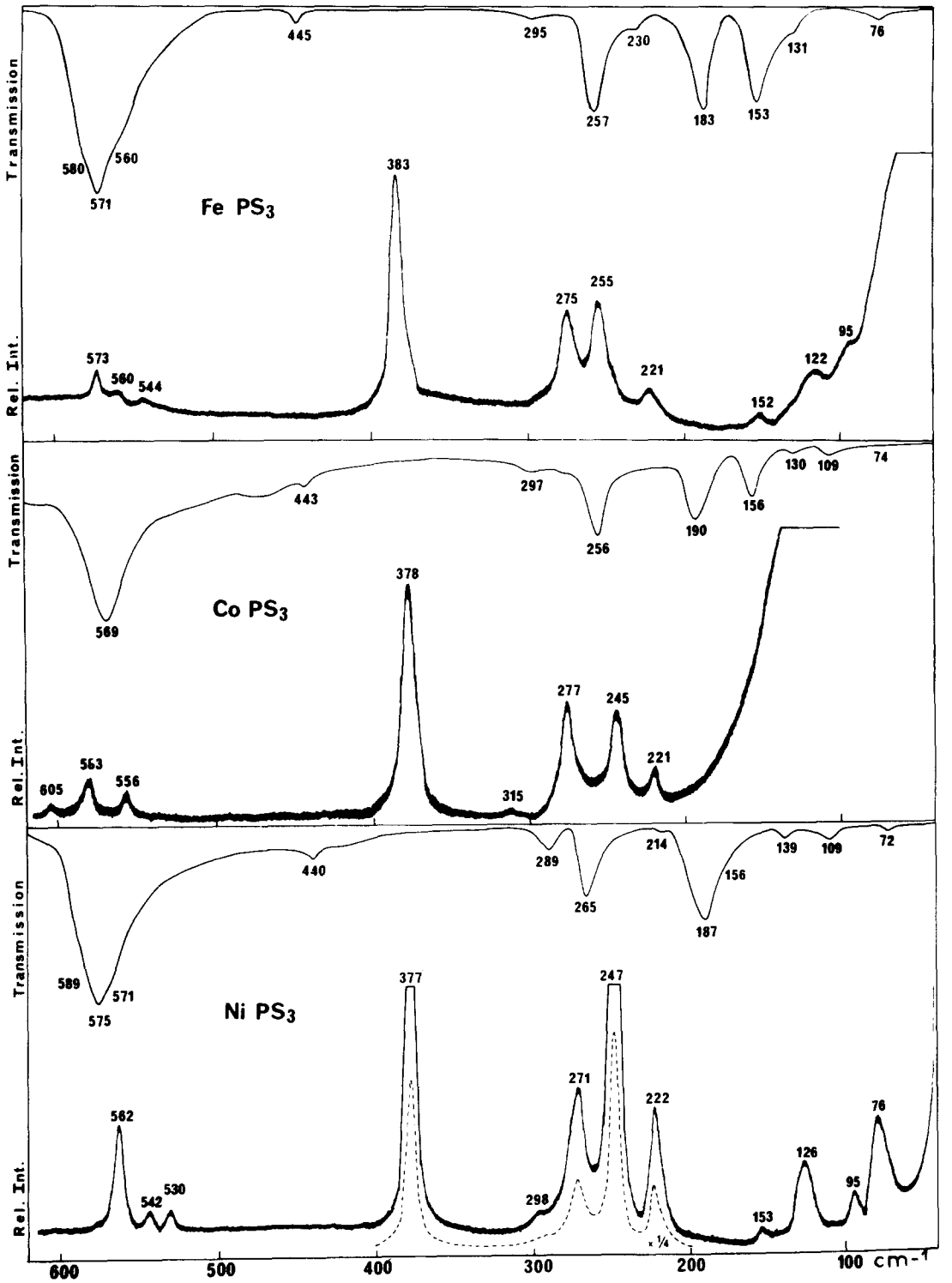

FIG. 3. Room temperature infrared and Raman spectra [620–10 cm^{-1}] of $FePS_3$, $CoPS_3$, and $NiPS_3$ compounds.

ations, the intensities of the bands at 445 cm^{-1} (ν(P–P)) and at 297 cm^{-1} ($\delta_s(PS_3)$) are also observed to decrease markedly.

III. Vibrational Spectra of the $In_{2/3}\square_{1/2}PS_3$ Compound

This metal vacancy compound, first characterized by Soled and Wold (*11*), is an insulator and has an optical absorption edge of 3.1 eV. According to Diehl and Carpentier (*12*) it belongs to the monoclinic space group $P_{2_1/a}(C_{2h})$ and its crystal structure was found to be a metal-deficient threefold ($a' = 3a_0$) superstructure of the $FePS_3$ type formed by the ordering of indium atoms and of metal vacancies. The unit cell multiplicity is $Z = 12$, i.e., one obtains the formula $In_8\square_4(PS_3)_{12}$ per primitive cell which is composed of two sets of four In^{3+} ions on general positions and of three sets of four PS_3 groups; within the first family of these groups two $[P_2S_6^{4-}]$ anions exist on C_i sites and within both of the other sets, four $[P_2S_6^{4-}]$ entities are localized on general positions. Therefore one expects a total number of 168 crystalline normal modes, i.e., 48 vibrations for the first set of PS_3 groups, 96 vibrations for the remaining ones, and 24 translational motions of indium ions. For such a structure a complex vibrational spectrum is to be expected; we thus concentrate mainly on the effects of the threefold ordered superstructure.

The infrared (at 300 and 100 K) and Raman (at 300 and 10 K) spectra of this compound are shown on Fig. 5 for the powder samples and on Fig. 4 for a monocrystalline platelet. The corresponding band wavenumbers and approximate assignments are reported in Table V. As expected, many band splittings are observed, and, in particular for the degenerate

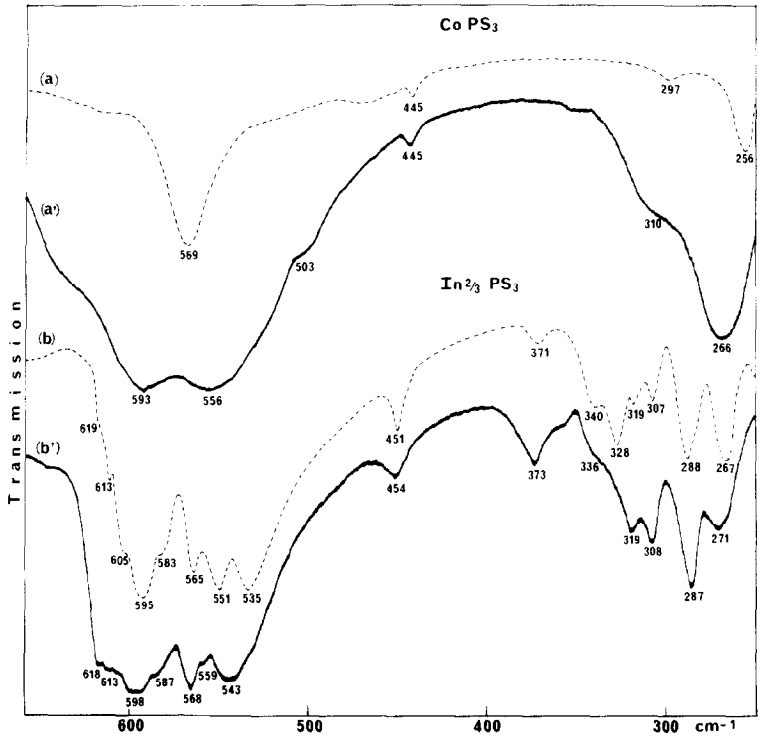

FIG. 4. Infrared spectra [650–250 cm^{-1}] of polycrystalline samples and of platelets for the same compound at 300 K: (a) and (a') for $CoPS_3$; (b) and (b') for $In_{2/3}\square_{1/3}PS_3$.

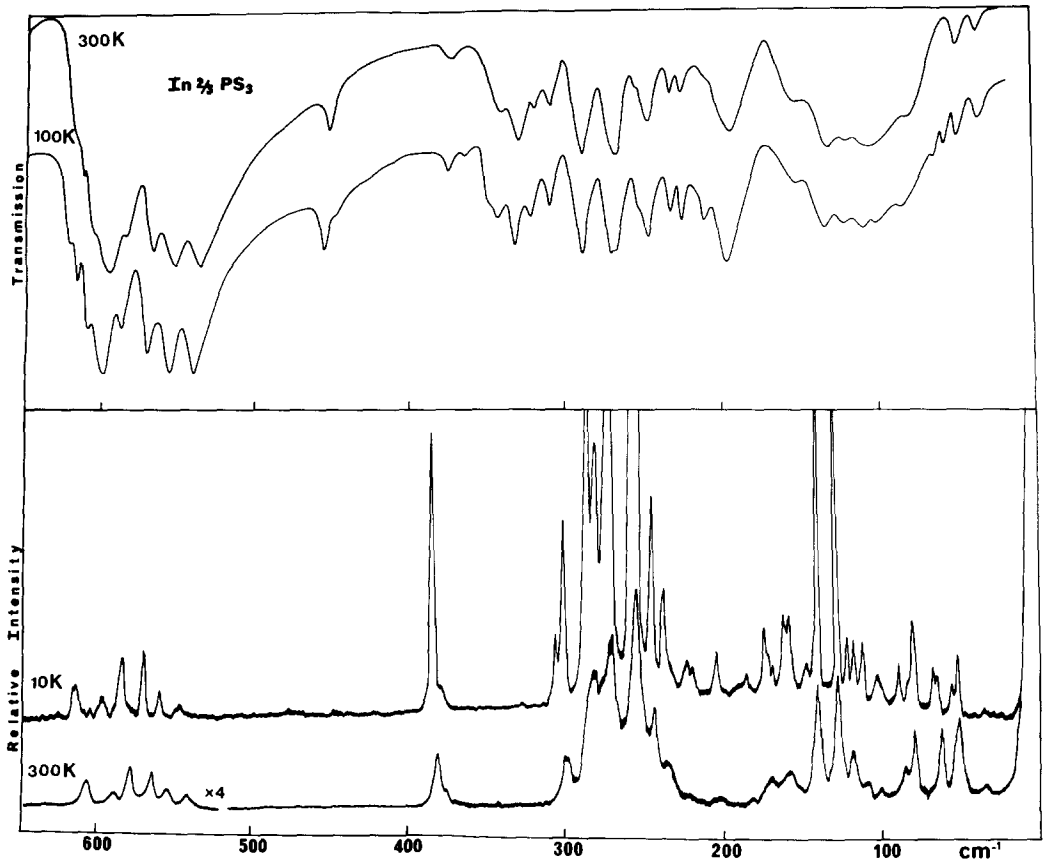

FIG. 5. Infrared (upper traces) and Raman (lower traces) spectra [650–10 cm^{-1}] of $In_{2/3}\square_{1/3}PS_3$ at room and low temperatures.

stretching vibrations of PS_3 groups, one observes nine infrared components and eleven Raman counterparts relative to the twelve expected in each case. We note again that the ν(P–P) vibration is only infrared active (at about 450 cm^{-1}) while the symmetric valence mode $\nu_s(PS_3)$ at about 380 cm^{-1} is essentially Raman active; the weak splittings of these modes show that the interlayer couplings are quite weak. Similarly, many low frequency bands at $\nu \leq$ 120 cm^{-1} assigned to $T'(In^{3+})$ motions are clearly resolved on the Raman spectrum at 10 K and small A_g–B_g splittings can also be observed. Nevertheless, the spectra do not change dramatically when cooling down the samples; we conclude, in agreement with the X-ray results (*11, 12*), that no phase transition occurs and that the superstructure is completely ordered at room temperature. Finally, the polarized infrared spectrum obtained with a platelet (Fig. 4) exhibits polarization effects similar to those described for $CoPS_3$: the intensities of the bands at 450 cm^{-1} (νP–P) and at 340–330 cm^{-1} (δ_sPS_3) decrease. However, intensities of the bands at 373 cm^{-1} (ν_sPS_3) and at 320–310 cm^{-1} (δ_sPS_3) increase markedly. In agreement with X-ray results (*12*), this shows that two families of ($P_2S_6^{4-}$) entities exist: the anions of the first family (localized on C_i sites) are responsible for the expected behavior of the two former bands, while those of the second family (on general positions) give rise to the particular polarization effects for the two latter bands.

From this we conclude that this last set of anions is built of nearly flat PS_3 pyramids which are tilted out of the (00*l*) layer planes.

IV. Infrared Spectra of $FePS_3$, $CoPS_3$, $NiPS_3$ Intercalated with $[CoCp_2^+]$

There are no accurate structural data for these intercalated compounds. X-Ray powder diagrams have shown that an interlayer distance increase of 5.3 to 5.4 Å takes place upon intercalation (*2, 16*) but no superstructure is in evidence among the (00*l*) lines. However, the chemical composition MPS_3–$(CoCp_2)_x$ with $x \simeq 1/3$ suggests that the primitive unit cell can have at least a threefold multiplicity. The infrared spectra (700–30 cm^{-1}) of these compounds at 300 and 100 K are shown on Fig. 6 where they are compared with those previously obtained for the manganese derivative (*4*). All the band wavenumbers are collected in Table IV. As these compounds are extremely opaque, we have not been able to obtain Raman data.

The infrared spectra of these intercalates do not exhibit large changes with respect to those of the host lattices but new bands clearly appear:

Some of these are characteristic of the $(CoCp_2^+)$ cationic species demonstrating that an electron transfer from the organometallic species to the host lattice has occurred during the intercalation reaction. More precisely, tilting, asymmetric stretching, and deformation via metal–ligand vibrations are observed at about 500, 460, and 175 cm^{-1}, respectively. We have also observed some internal vibrations of the Cp rings, in particular the out-of-plane γ(C–H) modes at about 860 cm^{-1}. All the above mentioned bands still appear with strong intensity in the polarized infrared spectrum (**E**//*ab*) as recorded with a platelet of the iron compound (Fig. 6). We again conclude (*4*) that the C_5 symmetry axis of the guest cations lies parallel to the host lattice layers.

In the high frequency region, 650–550 cm^{-1}, other absorption bands due to the host lattice are greatly altered: the asymmetric stretching modes $\nu_d(PS_3)$ are split into at least five broad components indicating that some distortion of the PS_3 groups

TABLE V

INFRARED AND RAMAN BAND WAVENUMBERS (cm^{-1}) OF THE METAL-DEFICIENT $In_{2/3}\square_{1/3}PS_3$ COMPOUND

Infrared		Raman		
300 K	100 K	300 K	10 K	Approximate type of motions
619 sh	621 sh		625 vw	$\nu_d(PS_3)$
			617 w	
613 s	617 s		614 w	
605 s	609 s	608 w	604 vw	
595 s	598 vw		600 vw	
583 vw	586 s	590 vw	596 w	
			584 m	
565 vw	568 vw	570 w	570 m	
		565 w	559 w	
551 vw	554 vw	556 vw	548 vw	
535 vw	538 vw	542 w	545 vw	
	526 sh			
451 m	453 m	—	—	$T'_z(PS_3)$ or (P–P)
	445 w			

TABLE V—*Continued*

Infrared		Raman		
300 K	100 K	300 K	10 K	Approximate type of motions
			383 s	
371 w	373 w	379 s	382 sh	$\nu_s(PS_3)$
	363 vw	375 sh	376 w	
	347 sh			
340 m	342 m			
328 s	331 s			$\delta_s(PS_3)$
319 m	321 m			
307 m	309 m			
			305 m	
		299 s	300 s	
288 s	289 s	282 sh	286 s	
		280 s	280 s	
			276 sh	
	279 s	270 s	273 vw	$\delta_d(PS_3)$
267 s	267 s			
253 vw	252 sh	254 vw	256 vs	
245 m	246 m	243 s	244 s	
231 m	232 m	235 m	237 s	
			232 sh	
224 m	224 m		223 m	
		220 w	219 m	
208 vw	210 m			
192 s	195 s	202 w	204 m	
		183 w	186 w	ρr or $R'_{xy}(PS_3)$
			182 vw	
			173 m	
		169 m	168 w	
			161 m	
		158 m	158 m	
150 m	150 m		147 w	
131 s	132 s	139 s	140 s	$\delta_s(PS_3)$
		126 m	127 s	
			121 m	
118 s	119 s	117 m	117 m	
	108 s	110 w	111 m	
			103 m	
101 s	99 s	100 w	100 w	
		87 m	88 m	
78 m	84 m		83 m	$T'(In^{3+})$ + Corner Brillouin zone
		78 m	80 m	Lattice modes
			67 m	
	63 m	62 m	64 m	
			59 vw	
	53 m		55 m	
46 m	47 m	50 m	51 m	
34 w	35 w	34 w	35 w	
			25 vw	

has taken place. This cannot be directly accounted in terms of an electronic localization on the P–S bonds since a quite similar behavior has been noted (see above) for the indium host lattice; moreover, we do not observe any splitting of these bands on the infrared spectra of the lithium intercalates of $FePS_3$ and $NiPS_3$ (*27*). Hence, these broad and complex absorption bands (extending over somewhat 100 cm^{-1}) more than likely reflect the formation of a distorted structure or superstructure upon $CoCp_2$ intercalation. It should be mentioned here that such an interpretation is strongly supported by recent results obtained for the Mn derivative by Clement *et al.* (*28–29*): the combination of EXAFS data, magnetic susceptibility, and magnetization measurements clearly shows that the intercalation process induces a local disorder around the manganese ions. This disorder could be responsible for the intense spontaneous magnetization observed at low temperature (*29*).

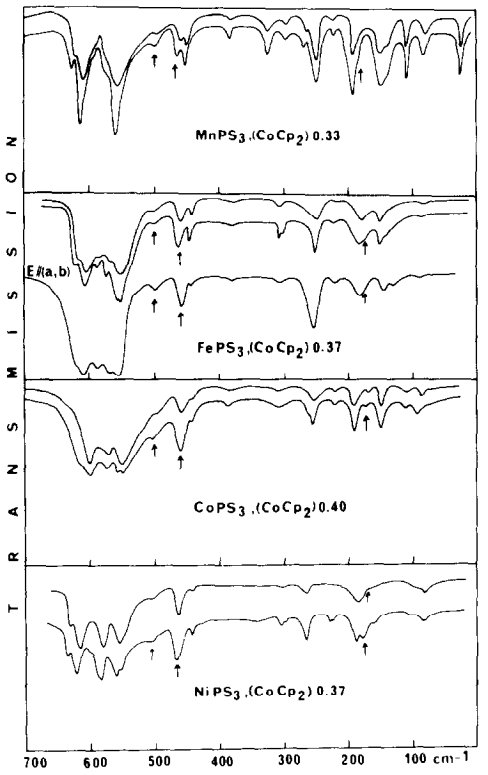

FIG. 6. Infrared spectra (700–30 cm^{-1}) of the ($CoCp_2^+$) intercalation compounds in $MnPS_3$, $FePS_3$, $CoPS_3$, and $NiPS_3$ at 300 K (upper traces) and at 100 K (lower traces). The polarized infrared spectrum of an intercalated platelet of $FePS_3$ at 300 K is given for comparison. Arrows indicate bands due to metal–ligand vibrations of $CoCp_2^+$.

In other respects, it is noteworthy that the average frequencies for these $\nu_d(PS_3)$ vibrations show an increase of 10 to 15 cm^{-1} upon intercalation suggesting a strengthening of some P–S bonds.

The most puzzling changes in the spectra concern the ν(P–P) modes whose frequencies are unaltered but whose relative intensities decrease markedly on passing from the manganese or iron to cobalt and nickel intercalates. This behavior may be related to the properties of the additional electrons gained by the host lattices during the intercalation process. As previously proposed by Johnson (*30*), we can correlated the decrease in the ν(P–P) intensity, observed in the case of Co and Ni compounds, with the location of the transferred electrons in the antibonding orbitals of some P_2 pairs. Indeed the reduction of some phosphorus atoms from the formal valence state of four to three would result in the breakdown of the corresponding P–P bonds and lead to the decrease of the ν(P–P) intensity; simultaneously a strengthening of the corresponding P–S bonds would be expected. Such a mechanism for the intercalation of cobaltocene in $CoPS_3$ and $NiPS_3$ host systems, where the P–P bonds behave as the main site of reduction, is in agreement with preliminary NMR results (*31*) which have shown that, when cobaltocene is intercalated in $NiPS_3$ both the position and the linewidth of the ^{31}P line are affected. One should recall that (i) this situation is in sharp contrast with the one encountered after Li intercalation in the same host lattice (*32, 33*); (ii) from optical and magnetic sus-

TABLE VI

INFRARED BAND WAVENUMBERS (cm^{-1}) OF $FePS_3$, $CoPS_3$, AND $NiPS_3$ INTERCALATED WITH $CoCp_2$

$FePS_3$-$(CoCp_2)_{0.37}$		$CoPS_3$-$(CoCp_2)_{0.39}$		$NiPS_3$-$(CoCp_2)_{0.37}$		Approximate type of motions
300 K	100 K	300 K	100 K	300 K	100 K	
1412 m	1413 m	1412	1413 m	1411 m	1411 m 1407 sh	νC–C of $CoCp_2^+$
1007 w	1007 w 1004 w	1007 w	1009 w	—	1007 w	δC–H $CoCP_2^+$
861 m	868 sh 860 m 848 sh	860 m	861 m 842 w	860 m	861 m	γCH $CoCp_2^+$
616 sh 603 vw 585 sh 570 s 552 vw	621 s 608 vw 588 s 575 s 562 vs 556 vs	615 sh 601 vs 574 s 553 vs	619 s 604 vs 577 s 560 vs 552 vs	626 sh 612 vs 576 vs 553 vs 545 sh	631 s 618 vs 599 m 585 sh 581 vs 558 vs 550 s	$\nu_d(PS_3)$
500 w	502 w	501 w	504 m	499 w	504 w	$Tilt_d$ $CoCp_2^+$
461 m	464 m	459 m	464 m	460 m	464 m	ν_{as} $CoCp_2^+$
445 m	448 m	443 m	446 w	437 vw	440 w	ν(P–P) or $T_z'^0(PS_3)$
378 vw	380 w	382 vw	384 w	380 vw	382 vw	$\nu_s^p(PS_3)$
306 m	308 m 305 w	308 vw	309 w	298 vw	300 w 294 vw	$\delta_s^0(PS_3)$
252 m	254 m 250 sh	253 m	255 sh 253 m	261 m	263 m	$\delta_d^0(PS_3)$
225 vw	226 vw	221 w	222 w	225 w	226 w 221 sh	ρr or $R_{xy}'(PS_3)$
180 m	186 m	185 m	187 m	179 m	186 m	
172 vw	175 m	170 w	172 w	172 vw	174 m	Def. $CoCp_2^+$
151 m	152 m	146 m	146 m	154 vw	156 w	$\delta_s^p(PS_3)$
144 vw	145 vw			—	—	
		115 w	115 w	90 sh	92 w	$T'M^{2+}$
82 vw	83 w	84 m	85 m	77 m	78 m	

ceptibility measurements it was already concluded that the ligand field around the nickel ions increases upon $CoCp_2$ intercalation and that the nickel ions are not reduced (*16*).

Concerning the cobaltocene intercalate of $FePS_3$, as no decrease is observed in ν(P–P) intensities and as no ^{31}P-NMR results are yet reported, it is impossible to ascertain whether the previous mechanism is still operative; therefore another kind of electronic transfer, based on the reduction of some transition metal cations, cannot be ruled out. In this respect studies in the far infrared region of the T' modes of metal ions should be highly informative. In fact, we observe two very weak bands at 114 and 82 cm^{-1}. Two bands are also detected in the same region with the cobalt and nickel intercalates but it should be noted that the relative intensities of the lowest frequency bands (at 82, 84, and 77 cm^{-1}, respectively), increase when going from the iron to the cobalt and nickel derivatives. The lower intensity of the T'_{Fe} mode might suggest that some iron cations were reduced upon co-

baltocene intercalation; therefore, a mechanism distinct from the one depicted in Co and Ni intercalates could be involved with the Fe compound.

Conclusion

In this spectroscopic study, a new assignment for the vibrational modes of $P_2S_6^{4-}$ anions (D_{3d} symmetry) has been postulated and the infrared and Raman spectra of the lamellar MPS_3 compounds with M = Fe, Co, Ni, $In_{2/3}$ have been analyzed for the first time. From the infrared spectra of the $Co(C_5H_5)_2^+$ intercalated host lattices under study a mechanism for the electronic transfer during the intercalation process has been proposed: the main reduction site for $CoPS_3$ and $NiPS_3$ compounds is the P–P bond, while some reduction of iron ions in $FePS_3$ cannot be ruled out.

Studies of the lithium intercalates of $FePS_3$ and $NiPS_3$ are currently in progress in order to obtain additional structural and spectrospic information and to check if distinct mechanisms are also operative for the electron transfer accompanying Li intercalation in Fe and Ni analogs.

Acknowledgments

The authors thank Mrs. M. Revault for technical assistance in far-infrared measurements, Dr. P. Dhamelincourt for some experiments with the Mole instrument, and Dr. R. Clément, Professor G. Lucazeau, and Professor J. Rouxel for helpful discussions. This work was supported by CNRS (ATP Chimie Fine).

References

1. R. Brec, D. M. Schleich, G. Ouvrard, A. Louisy, and J. Rouxel, *Inorg. Chem.* **18,** 1814 (1979).
2. R. Clément, and M. L. H. Green, *J. Chem. Soc. Dalton Trans.* **10,** 1566 (1979).
3. A. Le Méhauté, G. Ouvrard, R. Brec, and J. Rouxel, *Mater. Res. Bull.* **12,** 1191 (1977).
4. Y. Mathey, R. Clément, C. Sourisseau, and J. Lucazeau, *Inorg. Chem.* **19,** 2773 (1980).
5. C. Sourisseau, J. P. Forgerit, and Y. Mathey, *J. Phys. Chem. Solids* **44,** 119 (1983).
6. C. Sourisseau, Y. Mathey, and C. Poinsignon, *Chem. Phys.* **71,** 257 (1982).
7. C. Sourisseau and Y. Mathey *in* "Proceedings, 8th International Conference on Raman Spectroscopy" Bordeaux (J. Lascombe and Pham. V. Huong, Eds.), p. 641, Wiley, New York (1982).
8. O. Poizat, J. Belloc, C. Sourisseau, R. Clément, and Y. Mathey, *in* "Proceedings, 8th International Conference on Raman Spectroscopy" Bordeaux (J. Lascombe and Pham. V. Huong Eds.), p. 639, Wiley, New York (1982).
9. R. Brec, D. Schleich, A. Louisy, and J. Rouxel, *Ann. Chim. Fr.* **3,** 347 (1978).
10. R. Brec, G. Ouvrard, A. Louisy, J. Rouxel, and A. Le Méhauté, *Solid State Ionics* **6,** 185 (1982).
11. S. Soled and A. Wold, *Mater. Res. Bull.* **11,** 657 (1976).
12. R. Diehl and C. D. Carpenter, *Acta Crystallogr. B* **34,** 1097 (1978).
13. H. Falius, *Z. Anorg. Allg. Chem.* **356,** 189 (1968).
14. W. Klingen, R. Ott, and H. Hahn, *Z. Anorg. Allg. Chem.* **396,** 271 (1973).
15. G. Ouvrard, R. Brec, and J. Rouxel, *C.R. Acad. Sci Ser. II* **294,** 971 (1982).
16. R. Clément, O. Garnier, and Y. Mathey, *Nouv. J. Chim.* **6,** 13 (1982).
17. R. Clément, *J. Chem. Soc. Chem. Commun.* 647 (1980).
18. H. Burger and H. Falius, *Z. Anorg. Allg. Chem.* **363,** 24 (1968).
19. R. Mercier, J. P. Malugani, B. Fahys, J. Douglade, and G. Robert, *J. Solid State Chem.* **43,** 151 (1982).
20. F. Hoffer, W. Sawodny, and E. Hengge, *Spectrochim. Acta A* **26,** 819 (1970).
21. H. Burger, G. Pawelke, and H. Falius, *Spectrochim. Acta A* **37,** 753 (1981).
22. C. W. F. T. Pistorius, *J. Chem. Phys.* **29,** 1421 (1959).
23. G. K. Somayajulu, *J. Chem. Phys.* **28,** 814 (1958).
24. W. Klingen, G. Eulenberger, and H. Hahn, *Z. Anorg. Allg. Chem.* **401,** 97 (1973).
25. V. P. Zakharov and V. S. Gerasimenko, "Structural Features of Semiconductors in the Amorphous State," Naukova Dumka, Kiev (1976).
26. M. I. Gurzan, A. P. Buturlakin, V. S. Gerasimenko, N. F. Korda, and V. Yu Slivka, *Sov. Phys. Solid State (Engl. Transl.)* **19,** 1794 (1977).
27. M. Barj, C. Sourisseau, G. Ouvrard, and R. Brec, *Solid State Ionics* (1983), in press.

28. A. MICHALOWICZ AND R. CLÉMENT, *Inorg. Chem.* **21,** 3872 (1982).

29. R. CLÉMENT, J. P. AUDIERE, AND J. P. RENARD, *Rev. Chim. Miner.* **19,** 560 (1982).

30. J. W. JOHNSON *in* "Intercalation Chemistry" (M. S. Whittingham and A. J. Jacobson, Eds.), Academic Press, New York (1982).

31. J. W. JOHNSON AND B. G. SILBERNAGEL, unpublished results.

32. C. BERTHIER, Y. CHABRE, AND M. MINIER, *Solid State Commun.* **28,** 327 (1978).

33. Y. CHABRE, P. SEGRANSAN, C. BERTHIER, AND G. OUVRARD, "Fast Ion Transport in Solids," p. 221, Lake Geneva, Wisconsin (1979).